GEOLOGICAL
SURVEY
OF
CANADA

DEPARTMENT OF ENERGY,
MINES AND RESOURCES

PAPER 71-18

SECONDARY FIELDS OF A VERTICAL MAGNETIC DIPOLE ABOVE A THIN HORIZONTAL LAYER OF CONDUCTIVE OVERBURDEN

(Report and 8 figures)

A. V. Dyck and A. Becker

Price, $1.50

1971

GEOLOGICAL SURVEY
OF CANADA

PAPER 71-18

SECONDARY FIELDS OF A VERTICAL MAGNETIC DIPOLE ABOVE A THIN HORIZONTAL LAYER OF CONDUCTIVE OVERBURDEN

A. V. Dyck and A. Becker

DEPARTMENT OF ENERGY, MINES AND RESOURCES

Available by mail from *Information Canada*, Ottawa

from the Geological Survey of Canada
601 Booth St., Ottawa

and

Information Canada bookshops in

HALIFAX - 1735 Barrington Street
MONTREAL - 1182 St. Catherine Street West
OTTAWA - 171 Slater Street
TORONTO - 221 Yonge Street
WINNIPEG - 499 Portage Avenue
VANCOUVER - 657 Granville Street

or through your bookseller

Price: $1.50 Catalogue No. M44-71-18

Price subject to change without notice

Information Canada
Ottawa
1971

CONTENTS

Illustrations

ABSTRACT

A detailed numerical calculation of the secondary magnetic field due to a vertical magnetic dipole above a thin horizontal conductor reveals this quantity to be elliptically polarized. The current distribution in the conductive sheet is circular and sharply bounded so that about 97 per cent of the induced current is contained by a circular region whose radius approximately equals five times the height of the source above the conductor.

The mathematical thin sheet model is most useful for the calibration of EM scale-model equipment. Its validity for the interpretation of survey data however, is limited.

RÉSUMÉ

A la suite du calcul numérique détaillé du champ magnétique secondaire occasioné par un bipole magnétique vertical au-dessus d'un mince conducteur horizontal, l'auteur a déterminé que le champ était polarisé de manière elliptique. La diffusion du courant à l'intériur de la couche conductrice est circulaire et nettement délimitée de façon qu'environ 97 p. 100 du courant induit se trouve maintenu à l'intérieur d'une zone circulaire dont le rayon équivaut approximativement à cinq fois la hauteur de la source au-dessus du conducteur.

Le modèle mathématique de couche mince est de grande utilité pour l'étalonnage de l'équipement électromagnétique expérimental mais son emploi est limité dans l'interprétation des données de levés.

SECONDARY FIELDS OF A VERTICAL MAGNETIC DIPOLE ABOVE A THIN HORIZONTAL LAYER OF CONDUCTIVE OVERBURDEN

INTRODUCTION

The recognition of overburden effects in the results of an electromagnetic prospecting survey is essential to the separation and identification of surficial and deeper conductors. On the other hand, the interpretation of EM surveys carried out for the explicit purpose of mapping surficial deposits requires detailed theoretical knowledge of the secondary field behaviour over stratified formations.

This paper presents a numerical evaluation of the secondary fields produced by an oscillating vertical magnetic dipole located above a thin, horizontal conducting sheet. This mathematical model is of course only an approximation to real situations where the conductive layer has finite thickness. The thin-sheet model however, is most useful for the calibration of electromagnetic scale models. In this case a comparison of theoretical and scale-model data yields immediately an estimate of the accuracy of the scale-model instrumentation.

The theoretical aspects of the thin-sheet problem have been treated by Wait (1953) and by Grant and West (1965). The thin-sheet model has more recently been used by Duckworth (1970) in performing depth determinations with a two coplanar coil configuration. While the analytical formulae for the secondary electromagnetic field are fairly simple, their evaluation is rather difficult because of the presence of Bessel functions in the associated unbounded integrals. It is thus imperative to employ numerical quadrature techniques on a high-speed digital computer.

The results are tabulated and presented graphically as a function of the system geometry and the ratio of the sheet thickness to the skin depth (in the conductor) of the primary excitation. A comparison of this data with the results published previously by Frischknecht (1967) for a similar system above a two-layer earth enables us to establish the range of validity for the thin-sheet approximation to that problem.

It was also thought worthwhile to evaluate the induced current density distribution in the sheet. While this result is mainly of academic interest, it does however, permit us to estimate the minimum lateral extent of a thin-sheet conductor which is necessary before the "infinite sheet" theory, considered here, becomes applicable to a flat-lying, tabular body, of finite size.

Original manuscript submitted: January 8, 1971
Final version approved for publication: February 19, 1971

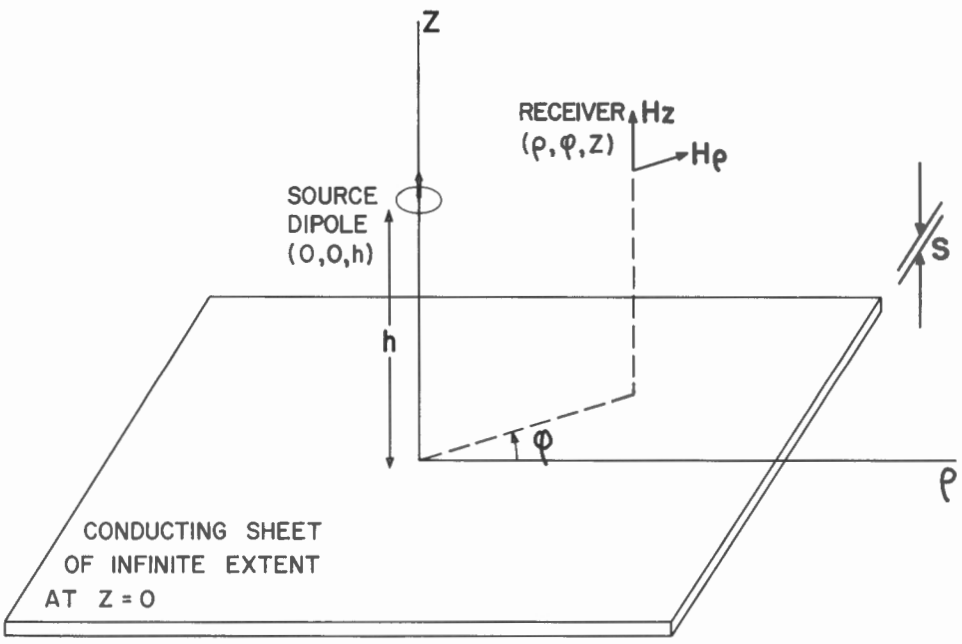

Figure 1. Vertical magnetic dipole situated over a horizontal sheet of infinite extent. The boundary value problem is solved in cylindrical co-ordinates (ρ, φ, Z).

THEORY

The formal solution to the problem of a magnetic dipole over a conducting sheet (Fig. 1) may be readily obtained by the method of Grant and West (1965, pp. 504, 505). Considerable simplification is achieved by neglecting displacement currents everywhere. If in addition to this, one assumes that the induced current is restricted to a horizontal plane then the solution of the problem is completed by applying the appropriate boundary condition (Grant and West, 1965, p. 499) to yield the vertical and horizontal components of the secondary field (Wait, 1953):

$$\frac{4\pi\rho^3}{m}\begin{Bmatrix} H_z^{(s)} \\ H_\rho^{(s)} \end{Bmatrix} = \int_0^\infty \frac{i\alpha a}{\lambda + i\alpha a}\, e^{-\lambda/a}\, \lambda^2 \begin{Bmatrix} J_0(\lambda) \\ J_1(\lambda) \end{Bmatrix} d\lambda \qquad (1)$$

where m = dipole moment = I dA
I = current in the loop
dA = area of the loop
β = z + h
q = $\sigma \mu_0 \omega s/2$
α = β q
a = ρ/β
and λ is the variable of integration.

These infinite integrals do not, in general, lend themselves to an analytical evaluation. Wait (1953) however, has derived simple expressions applicable either at very low frequencies ($\alpha \longrightarrow 0$, resistive limit) or at very high frequencies ($\alpha \longrightarrow \infty$, inductive limit). Allowing for a change in notation, these are:

$$\lim_{\alpha \longrightarrow \infty} \left[\frac{4\pi\rho^3}{m} H_z^{(s)} \right] = \frac{a\,(2-a^2)}{(a^2+1)^{5/2}} + \frac{i}{\alpha} \frac{a^3(6-9a^2)}{(a^2+1)^{7/2}}$$

$$\lim_{\alpha \longrightarrow 0} \left[\frac{4\pi\rho^3}{m} H_z^{(s)} \right] = \alpha^2 \frac{a^3}{\sqrt{a^2+1}} + i\alpha \frac{a^3}{(a^2+1)^{3/2}} \qquad (2)$$

$$\lim_{\alpha \longrightarrow \infty} \left[\frac{4\pi\rho^3}{m} H_\rho^{(s)} \right] = \frac{3a^4}{(a^2+1)^{5/2}} + \frac{i}{\alpha} \frac{a^4(12-3a^2)}{(a^2+1)^{7/2}}$$

$$\lim_{\alpha \longrightarrow 0} \left[\frac{4\pi\rho^3}{m} H_\rho^{(s)} \right] = \alpha^2 \frac{a^2\left(\sqrt{a^2+1}-1\right)}{\sqrt{a^2+1}} + i\alpha \frac{a^4}{(a^2+1)^{3/2}} \qquad (3)$$

The precise range of validity for these expressions can best be determined by comparing the values they yield with those obtained numerically (Appendix). For example the useful range for a = 1 is indicated in Figures 2 and 3.

Numerical Details

A modified version of a U. S. Geological Survey computer program (Frischknecht, 1967) was used to evaluate the required integrals (1). Since the integrand is of an oscillatory nature the program computes separately the contribution of each segment bounded by the integrand zeros. The infinite integral is thus replaced by an infinite series of finite integrals of the form:

$$\int_0^\infty \varphi(a,\alpha,\zeta)\, J_n(\zeta)\, d\zeta = \sum_{i=1}^{\infty} \int_{x_{i-1}}^{x_i} \varphi(a,\alpha,\zeta)\, J_n(\zeta)\, d\zeta$$

$$= \sum_{i=1}^{\infty} A_i(a,\alpha)$$

Here, $x_0=0$, and x_i, i = 1, 2, 3, ---are the zeros of the Bessel function. The area of each segment, A_i, was determined using the 16-point Gaussian numerical integration procedure. Convergence of the series was established when A_i/A_1 became less than ϵ, a departure from the criterion described by Frischknecht (1967, p. 79). If the series had not converged by i = 40 then Euler's transformation (Hamming, 1962) was applied from i = 20 to i = 40 and the result added to $\sum_{i=1}^{20} A_i$

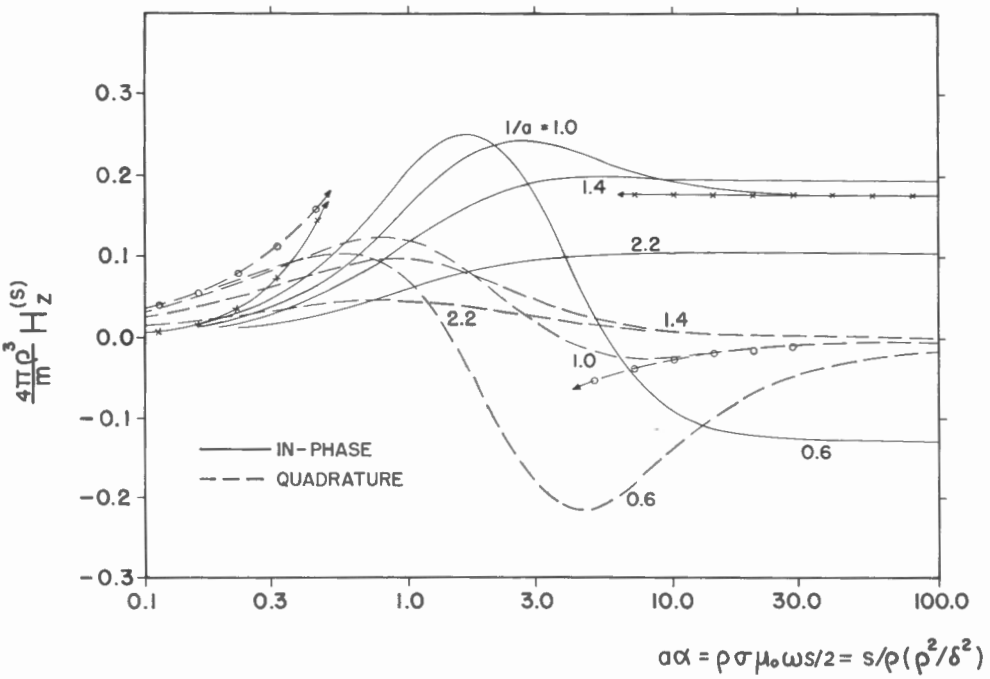

Figure 2. Frequency response of the vertical component of the secondary magnetic field. The value of $1/a = \rho/\beta$ is indicated for each pair of curves (in-phase and quadrature). For $1/a = 1.0$ the resistive and inductive limits as calculated from (2) are shown.

Five-to-six significant digit accuracy was obtained, using a value of $\epsilon = 10^{-6}$, for mid-range values of the parameters. However, difficulty was encountered for extreme values of ρ/β . Very large values of ρ/β (>20) produced such rapid oscillations of the integrand that the sum did not converge. Small values of ρ/β (<0.01) produced extremely long-period oscillations such that the only significant contribution to the integral came from the first segment, A_1. In this case it was found that the area of the first segment could be calculated more accurately by making use of the 32-point Gaussian quadrature rather than the 16-point method.

RESULTS

Frequency response

The normalized secondary magnetic field quantities $\frac{4\pi\rho^3}{m} H_z^{(s)}$ and $\frac{4\pi\rho^3}{m} H_\rho^{(s)}$ were calculated as a function of the parameter "a" and the variable $\alpha\alpha = \rho\sigma\mu_o\omega s/2$. The value of the parameter ranged from 0.01 to about 20 in steps of a factor of 2, while the variable "α" was incremented by

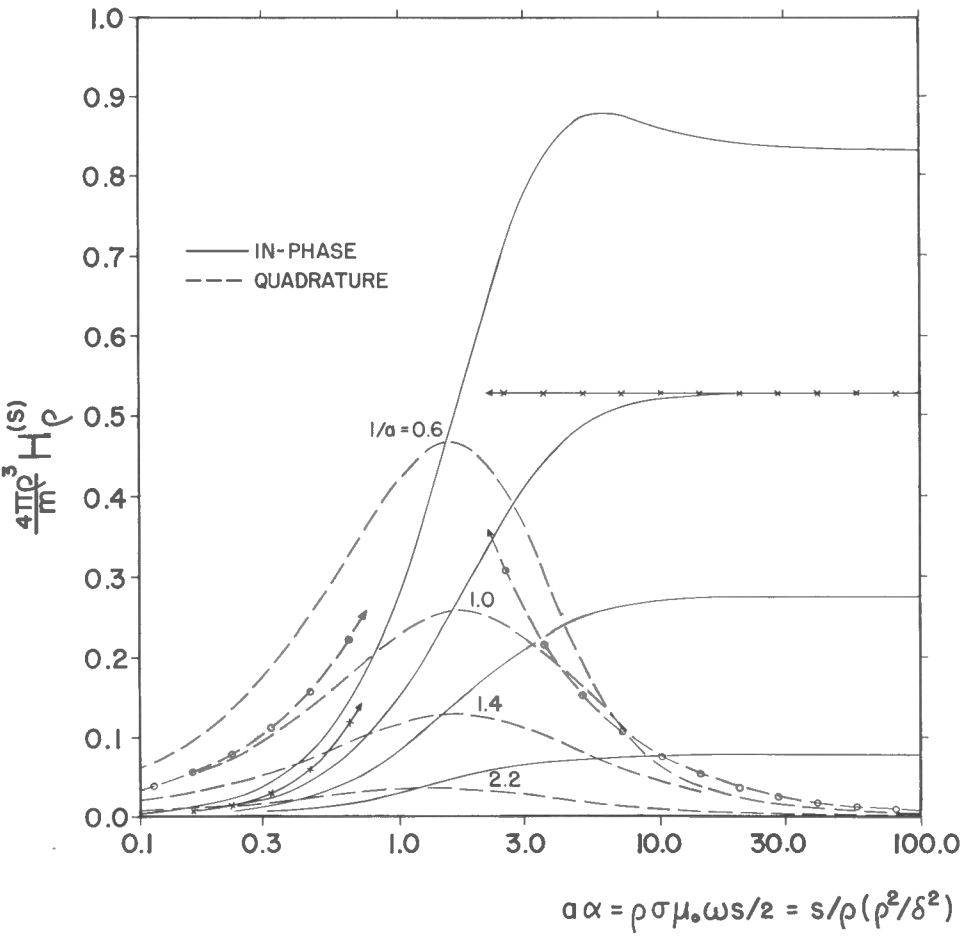

Figure 3. Frequency response of the horizontal component of the secondary magnetic field. The value of $1/a = \rho/\beta$ is indicated for each pair of curves (in-phase and quadrature). For $1/a = 1.0$ the resistive and inductive limits as calculated from (3) are shown.

a factor of $\sqrt{2}$ in the range from .005 to 58. A complete tabulation of the results is given in the Appendix, while typical results are displayed in Figures 2 and 3. One interesting feature which can be observed in these diagrams is the coincidence of the position of the maximum quadrature or imaginary response with the frequency at which the phase of the secondary field differs by 45° from that of the primary field.

Polarization of the secondary field

Examination of the secondary field components in the space around the source dipole shows that the horizontal and vertical components do not have the same phase. This leads to the conclusion that the secondary field

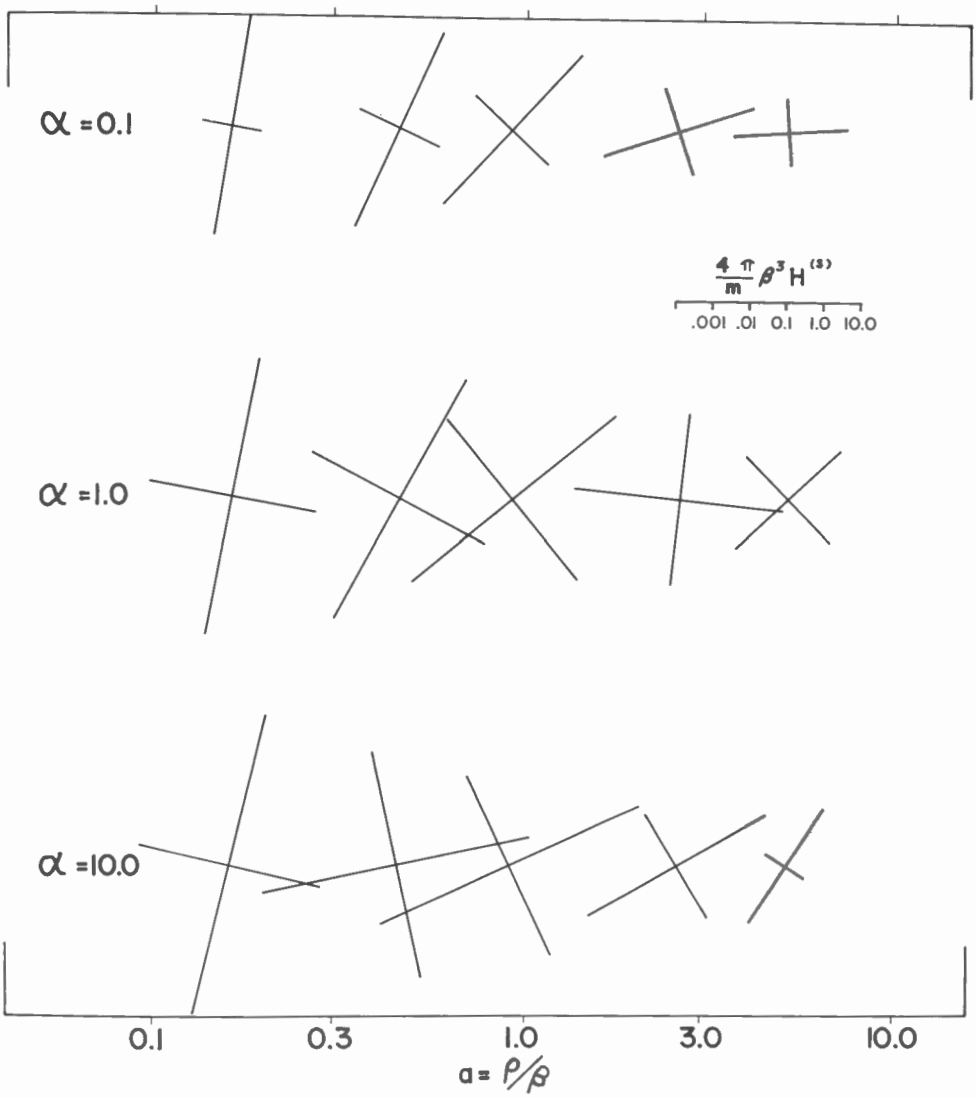

Figure 4. Elliptical polarization of the secondary magnetic field. The ellipse axes are drawn to a logarithmic scale as shown. One division of the scale represents a factor of 10.

is elliptically polarized. The axes and tilt-angles of the polarization ellipse were calculated for several values of α and several points in space.

The results are illustrated in Figure 4 with the ellipse axes plotted to a logarithmic scale as shown on the diagram. Since one division on the scale represents a factor of 10, it can be seen that, in most cases, the secondary field exhibits a high degree of ellipticity.

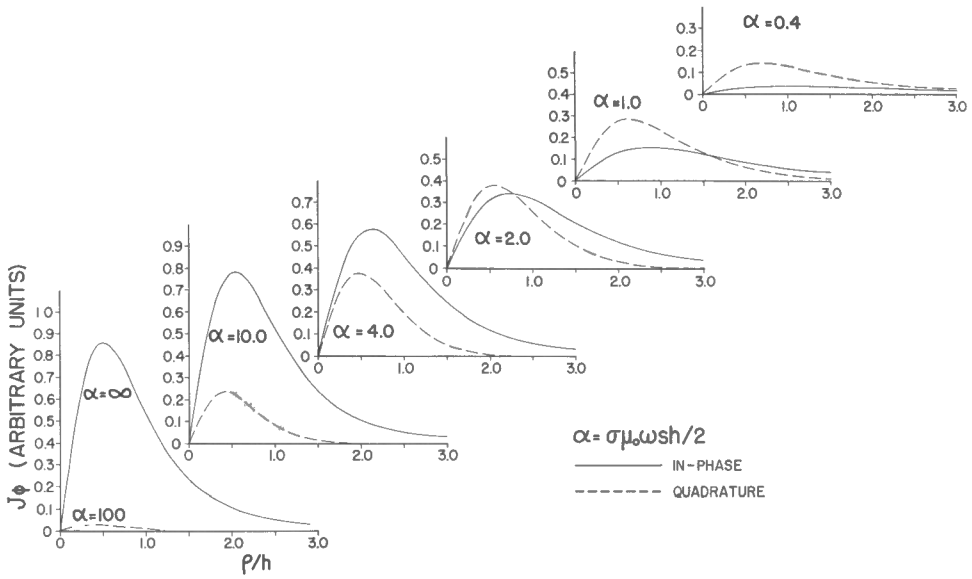

Figure 5. Horizontal distribution of eddy currents in the sheet.

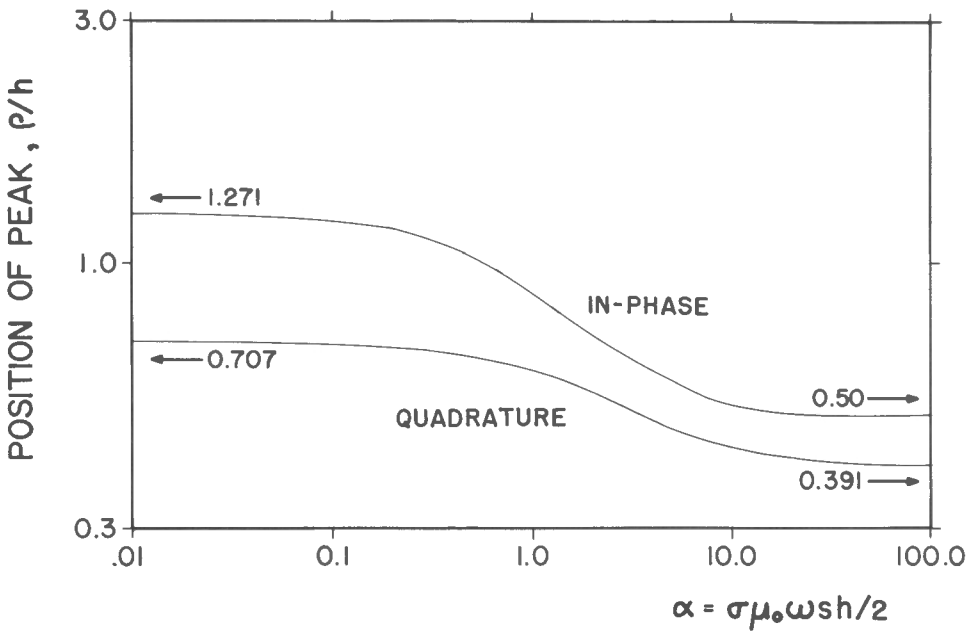

Figure 6. Variation in the peak of eddy current distribution. The peak positions for the resistive and inductive limits are indicated with arrows.

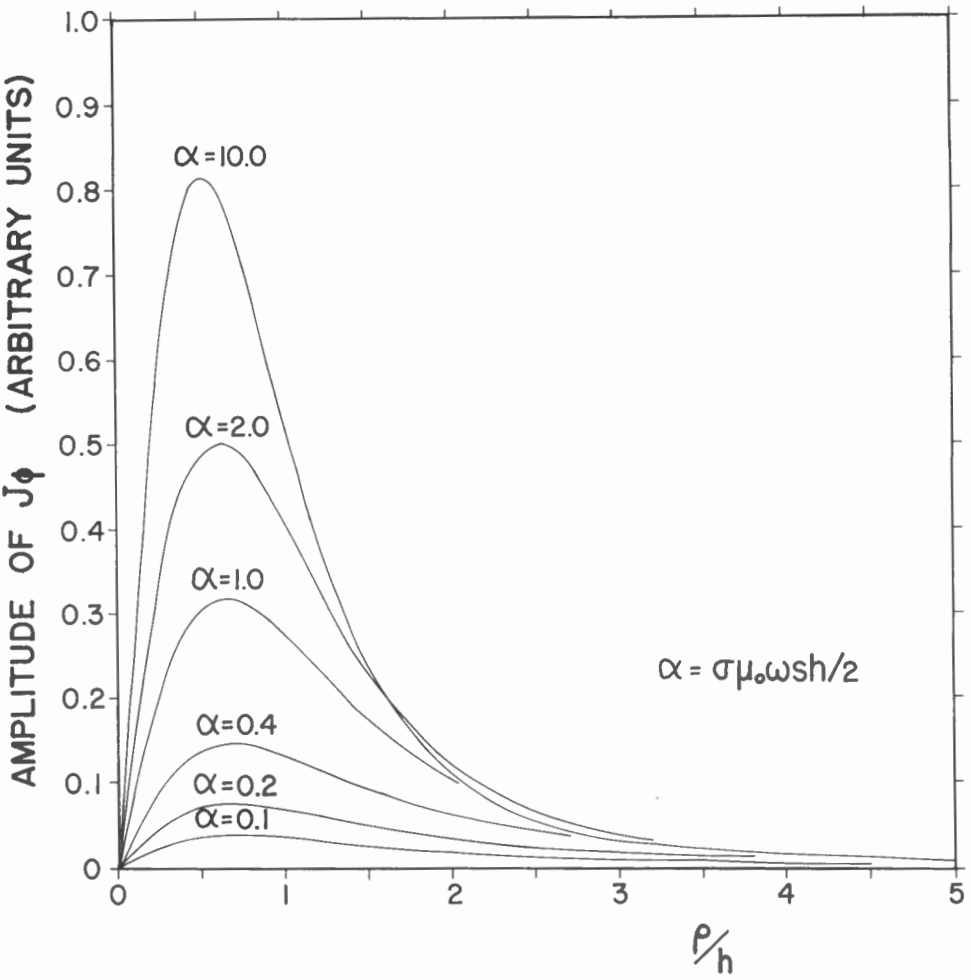

Figure 7. Amplitude of the complex eddy current distrubtion.

EDDY CURRENT DISTRIBUTION

The relationship between the tangential magnetic field, H_φ at any point on the surface of the sheet and the current density, J_φ, is given by $H_\varphi(\rho)\Big|_{z=0} = s/2\ J_\varphi(\rho)$ (Koefoed and Kegge, 1968). If one considers a current element a short distance away from the point of interest, P, it is obvious that the contribution of this current element to the magnetic field at P is entirely in the vertical direction because the sheet is thin. Therefore the tangential (or horizontal) component is due only to the current in the immediate vicinity of P.

Then for a given height, h, of the source dipole above the sheet, the eddy current distribution is proportional to the dimensionless response

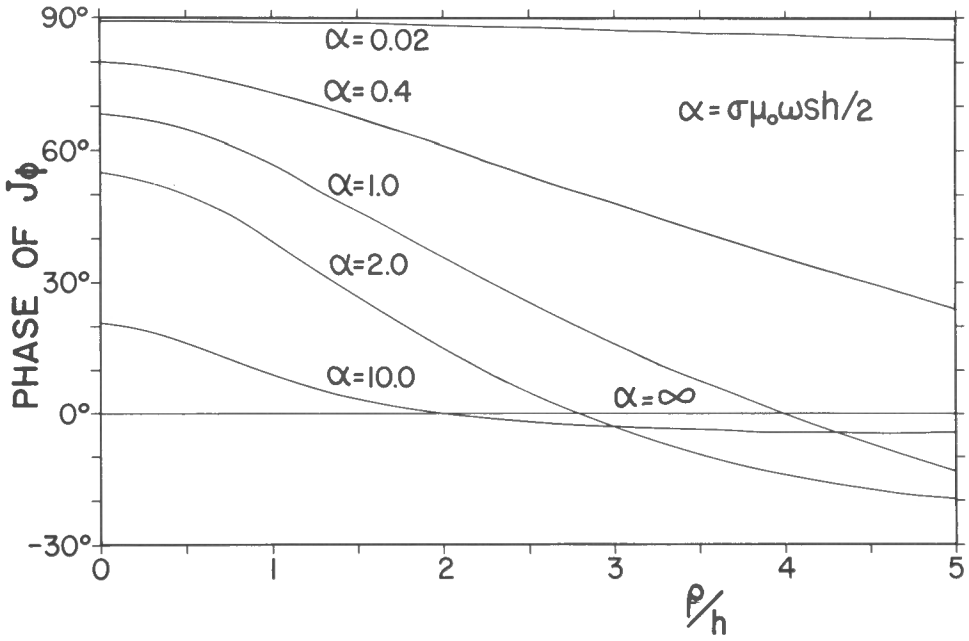

Figure 8. Phase of the complex eddy current distribution.

$\frac{4\pi h^3}{m} H_\rho^{(s)}$ (since z = 0, β = h). The eddy current distribution is plotted in arbitrary units in Figure 5 for several values of α. The graphs are presented in such a manner as to compare the in-phase and quadrature components of the current distribution and also to demonstrate the ring-like nature of the eddy currents. The flattening and enlarging of the rings as α decreases are also apparent from this graph. Notice that the rings of inphase current are larger than the rings of quadrature current. The positions of the peaks of the eddy current profiles are shown in Figure 6. Figure 7 is a graph of the total amplitude of the eddy currents in the same arbitrary units. In Figure 8, the phase of the induced current with respect to the primary field, clearly shows the change from a phase lag to a phase lead at a distance from the source dipole.

A rough calculation based on the contribution of annular segments of the eddy current distribution to the vertical secondary field component at ρ = 0 was made. It shows, for example, that a circular, thin disc whose radius, R, is such that R/h~ 5 will respond with approximately 97 per cent of the full response of a sheet of infinite extent for a value of α = 1.

VALIDITY OF THE THIN-SHEET HYPOTHESIS

The degree to which the thin-sheet model represents an actual situation where the conductor has finite thickness evidently depends on the validity of the physical assumption which defines this model. Here, the restriction of the induced current to a horizontal plane immediately implies

that the thickness of a physical model must be considerably smaller than either the dimension of the measuring system or the skin depth in the sheet material at the frequency in question.

The exact range of parameters for which the thin-sheet hypothesis is tenable can only be defined with reference to a particular component of the secondary field. Even then, the error caused by this hypothesis does not appear predictable a priori and must be determined by comparing the "thin-sheet" data with that computed for a sheet of finite thickness. The U.S. Geological Survey program (Frischknecht, 1967) can be modified to yield results for a conducting layer of any thickness. If for example one chooses the quadrature component of either the horizontal or the vertical secondary field as the error defining entity then it is found that the "thin-sheet" hypothesis is applicable, with an accuracy of about 5 per cent, to physical models whose thickness does not exceed either 1 per cent of the system dimension, $\left(\ell = \sqrt{(h^2+\rho^2)/2} \right)$ or 50 per cent of the skin depth in the material.

In practice, one encounters skin depths, in the overburden, which range from 5 to 500 metres while most EM systems have a characteristic dimension of about 100 metres. One must then conclude that the "thin-sheet" data is only valid for physical models whose thickness does not exceed one metre.

CONCLUSIONS

The results of a detailed numerical calculation of the secondary fields created by the presence of a vertical dipole source above a thin horizontal conducting sheet may be summarized as follows:

(a) The induction parameter value which yields maximum quadrature response for any one secondary field component is also approximately the value which yields a 45° phase shift for that component.

(b) The secondary field is elliptically polarized to a high degree of ellipticity.

(c) The current distribution in the sheet is annular with a well-defined maximum. The position of maximum current density is a function of the induction parameter; however, almost all the current is contained within a radius equal to five times the height of the source.

(d) The mathematical "thin-sheet" model can only be used to represent physical models whose thickness is very small when compared to the EM system dimensions.

The above summary leads us to conclude that, while thin horizontal sheets may be useful in the calibration of scale models, their utility for the simulation of overburden response (Lowrie and West, 1965) is limited. When used for calibration, the physical dimensions of the sheet need only be one order of magnitude larger than the dimensions of the EM system model.

In considering the physical significance of the results one is tempted to visualize the creation of the secondary fields by a single image of the source situated below the conductor. The single image concept however is valid only at high frequencies (Smythe, 1950, p. 403). At lower frequencies, the results presented here indicate that there is no such single image which would recede from its inductive (high frequency) limit position much as the time-domain model (Grant and West, 1965, p. 500) recedes to infinity with increasing time after the sudden application of a primary field.

REFERENCES

Duckworth, K.
1970: Electromagnetic depth sounding applied to mining problems; Geophysics, vol. 35, No. 6, pp. 1086-1098.

Frischknecht, F.C.
1967: Fields about an oscillating magnetic dipole over a two-layer earth, and application to ground and airborne electromagnetic surveys; Quart. Colo. School Mines, vol. 62, No. 1.

Grant, F.S., and West, G.F.
1965: Interpretation theory in applied geophysics; McGraw-Hill Book Company, New York.

Hamming, R.W.
1962: Numerical methods for scientists and engineers; McGraw-Hill Book Company, New York.

Koefoed, O., and Kegge, G.
1968: The electrical current pattern induced by an oscillating magnetic dipole in a semi-infinite thin plate of infinitesimal resistivity; Geophy. Prospecting, vol. 16, No. 1, pp. 144-158.

Lowrie, W., and West, G.F.
1965: The effect of a conducting overburden on electromagnetic prospecting measurements; Geophysics, vol. 30, No. 4, pp. 624-632.

Smythe, W.R.
1950: Static and dynamic electricity; McGraw-Hill Book Company, New York.

Wait, J.R.
1953: Induction in a conducting sheet by a small current-carrying loop; Appl. Sci. Res., Sec. B, vol. 3, pp. 230-236.

APPENDIX

COMPUTED FREQUENCY RESPONSE

Explanation of symbols:

A = ρ/β

ALPHA = $\sigma\mu_0\omega s(z+h)/2$

H(Z) = $\frac{4\pi\rho^3}{m} H_z^{(s)}$

H(RHO) = $\frac{4\pi\rho^3}{m} H_\rho^{(s)}$

A= 0.01

ALPHA	H(Z) REAL	H(Z) IMAG	H(RHO) REAL	H(RHO) IMAG
0.5000E-02	0.24995E-10	0.49990E-08	0.12522E-12	0.49658E-10
0.7071E-02	0.49983E-10	0.70693E-08	0.25043E-12	0.70227E-10
0.1000E-01	0.99937E-10	0.99965E-08	0.50081E-12	0.99313E-10
0.1414E-01	0.19976E-09	0.14134E-07	0.10015E-11	0.14044E-09
0.2000E-01	0.39906E-09	0.19981E-07	0.20023E-11	0.19860E-09
0.2828E-01	0.79631E-09	0.28234E-07	0.40021E-11	0.28080E-09
0.4000E-01	0.15854E-08	0.39864E-07	0.79940E-11	0.39695E-09
0.5657E-01	0.31428E-08	0.56197E-07	0.15948E-10	0.56093E-09
0.8000E-01	0.61778E-08	0.78988E-07	0.31738E-10	0.79203E-09
0.1131E 00	0.11958E-07	0.11043E-06	0.62866E-10	0.11167E-08
0.1600E 00	0.22548E-07	0.15300E-06	0.12344E-09	0.15700E-08
0.2263E 00	0.40906E-07	0.20932E-06	0.23873E-09	0.21967E-08
0.3200E 00	0.70960E-07	0.28217E-06	0.45115E-09	0.30502E-08
0.4525E 00	0.11876E-06	0.37496E-06	0.82850E-09	0.41912E-08
0.6400E 00	0.19530E-06	0.48980E-06	0.14823E-08	0.56837E-08
0.9051E 00	0.31705E-06	0.62098E-06	0.26030E-08	0.75645E-08
0.1280E 01	0.49779E-06	0.74775E-06	0.44751E-08	0.97481E-08
0.1810E 01	0.73359E-06	0.83869E-06	0.73686E-08	0.11891E-07
0.2560E 01	0.99894E-06	0.87071E-06	0.11262E-07	0.13401E-07
0.3620E 01	0.12625E-05	0.83997E-06	0.15661E-07	0.13785E-07
0.5120E 01	0.14978E-05	0.75509E-06	0.19874E-07	0.13012E-07
0.7241E 01	0.16847E-05	0.63422E-06	0.23424E-07	0.11406E-07
0.1024E 02	0.18158E-05	0.50238E-06	0.26104E-07	0.93749E-08
0.1448E 02	0.18982E-05	0.38074E-06	0.27912E-07	0.73015E-08
0.2048E 02	0.19458E-05	0.28012E-06	0.29010E-07	0.54663E-08
0.2896E 02	0.19717E-05	0.20239E-06	0.29628E-07	0.39895E-08
0.4096E 02	0.19853E-05	0.14473E-06	0.29958E-07	0.28688E-08
0.5793E 02	0.19922E-05	0.10294E-06	0.30129E-07	0.20462E-08

A= 0.02

ALPHA	H(Z) REAL	H(Z) IMAG	H(RHO) REAL	H(RHO) IMAG
0.5000E-02	0.19989E-09	0.39973E-07	0.19993E-11	0.79951E-09
0.7071E-02	0.39964E-09	0.56527E-07	0.39983E-11	0.11307E-08
0.1000E-01	0.79874E-09	0.79930E-07	0.79957E-11	0.15990E-08
0.1414E-01	0.15953E-08	0.11301E-06	0.15988E-10	0.22611E-08
0.2000E-01	0.31819E-08	0.15973E-06	0.31961E-10	0.31974E-08
0.2828E-01	0.63299E-08	0.22565E-06	0.63865E-10	0.45209E-08
0.4000E-01	0.12529E-07	0.31846E-06	0.12750E-09	0.63911E-08
0.5657E-01	0.24577E-07	0.44863E-06	0.25412E-09	0.90313E-08
0.8000E-01	0.47491E-07	0.63007E-06	0.50491E-09	0.12753E-07
0.1131E 00	0.89841E-07	0.88088E-06	0.99783E-09	0.17985E-07
0.1600E 00	0.16610E-06	0.12243E-05	0.19559E-08	0.25305E-07
0.2263E 00	0.30188E-06	0.16891E-05	0.37940E-08	0.35470E-07
0.3200E 00	0.54288E-06	0.23043E-05	0.72765E-08	0.49414E-07
0.4525E 00	0.96096E-06	0.30830E-05	0.13767E-07	0.68117E-07
0.6400E 00	0.16444E-05	0.39991E-05	0.25473E-07	0.92182E-07
0.9051E 00	0.26706E-05	0.49769E-05	0.45338E-07	0.12109E-06
0.1280E 01	0.40848E-05	0.58989E-05	0.76272E-07	0.15253E-06
0.1810E 01	0.58819E-05	0.66038E-05	0.12014E-06	0.18246E-06
0.2560E 01	0.79519E-05	0.69087E-05	0.17689E-06	0.20519E-06
0.3620E 01	0.10066E-04	0.67064E-05	0.24271E-06	0.21422E-06
0.5120E 01	0.11966E-04	0.60374E-05	0.30925E-06	0.20584E-06
0.7241E 01	0.13466E-04	0.50688E-05	0.36730E-06	0.18232E-06
0.1024E 02	0.14515E-04	0.40136E-05	0.41135E-06	0.15033E-06
0.1448E 02	0.15173E-04	0.30413E-05	0.44084E-06	0.11712E-06
0.2048E 02	0.15553E-04	0.22374E-05	0.45865E-06	0.87665E-07
0.2896E 02	0.15760E-04	0.16165E-05	0.46863E-06	0.63970E-07
0.4096E 02	0.15869E-04	0.11560E-05	0.47395E-06	0.45995E-07
0.5793E 02	0.15924E-04	0.82214E-06	0.47670E-06	0.32805E-07

A= 0.04

ALPHA	H(Z) REAL	H(Z) IMAG	H(RHO) REAL	H(RHO) IMAG
0.5000E-02	0.15975E-08	0.31921E-06	0.31959E-10	0.12769E-07
0.7071E-02	0.31926E-08	0.45139E-06	0.63914E-10	0.18058E-07
0.1000E-01	0.63755E-08	0.63825E-06	0.12781E-09	0.25537E-07
0.1414E-01	0.12713E-07	0.90231E-06	0.25554E-09	0.36113E-07
0.2000E-01	0.25281E-07	0.12752E-05	0.51078E-09	0.51067E-07
0.2828E-01	0.50026E-07	0.18012E-05	0.10204E-08	0.72205E-07
0.4000E-01	0.98190E-07	0.25416E-05	0.20364E-08	0.10207E-06
0.5657E-01	0.19058E-06	0.35808E-05	0.40567E-08	0.14425E-06
0.8000E-01	0.36554E-06	0.50334E-05	0.80584E-08	0.20371E-06
0.1131E 00	0.69483E-06	0.70522E-05	0.15945E-07	0.28734E-06
0.1600E 00	0.13111E-05	0.98275E-05	0.31386E-07	0.40442E-06
0.2263E 00	0.24430E-05	0.13567E-04	0.61314E-07	0.56695E-06
0.3200E 00	0.44436E-05	0.18451E-04	0.11823E-06	0.78917E-06
0.4525E 00	0.78071E-05	0.24565E-04	0.22312E-06	0.10854E-05
0.6400E 00	0.13178E-04	0.31798E-04	0.40829E-06	0.14654E-05
0.9051E 00	0.21269E-04	0.39647E-04	0.71876E-06	0.19254E-05
0.1280E 01	0.32573E-04	0.47087E-04	0.12070E-05	0.24342E-05
0.1810E 01	0.46976E-04	0.52703E-04	0.19117E-05	0.29206E-05
0.2560E 01	0.63498E-04	0.55086E-04	0.28268E-05	0.32825E-05
0.3620E 01	0.80343E-04	0.53444E-04	0.38796E-05	0.34195E-05
0.5120E 01	0.95472E-04	0.48090E-04	0.49386E-05	0.32822E-05
0.7241E 01	0.10741E-03	0.40356E-04	0.58628E-05	0.29065E-05
0.1024E 02	0.11575E-03	0.31942E-04	0.65644E-05	0.23960E-05
0.1448E 02	0.12098E-03	0.24197E-04	0.70339E-05	0.18663E-05
0.2048E 02	0.12400E-03	0.17797E-04	0.73174E-05	0.13967E-05
0.2896E 02	0.12564E-03	0.12856E-04	0.74761E-05	0.10191E-05
0.4096E 02	0.12650E-03	0.91931E-05	0.75607E-05	0.73268E-06
0.5793E 02	0.12694E-03	0.65380E-05	0.76045E-05	0.52255E-06

A= 0.08

ALPHA	H(Z) REAL	H(Z) IMAG	H(RHO) REAL	H(RHO) IMAG
0.5000E-02	0.12739E-07	0.25354E-05	0.50951E-09	0.20285E-06
0.7071E-02	0.25437E-07	0.35852E-05	0.10189E-08	0.28686E-06
0.1000E-01	0.50720E-07	0.50692E-05	0.20375E-08	0.40568E-06
0.1414E-01	0.10087E-06	0.71662E-05	0.40735E-08	0.57369E-06
0.2000E-01	0.19975E-06	0.10127E-04	0.81415E-08	0.81123E-06
0.2828E-01	0.39327E-06	0.14305E-04	0.16263E-07	0.11470E-05
0.4000E-01	0.76952E-06	0.20190E-04	0.32454E-07	0.16215E-05
0.5657E-01	0.14984E-05	0.28459E-04	0.64673E-07	0.22915E-05
0.8000E-01	0.29040E-05	0.40028E-04	0.12861E-06	0.32363E-05
0.1131E 00	0.55818E-05	0.56082E-04	0.25489E-06	0.45648E-05
0.1600E 00	0.10569E-04	0.78074E-04	0.50221E-06	0.64238E-05
0.2263E 00	0.19595E-04	0.10764E-03	0.97975E-06	0.90024E-05
0.3200E 00	0.35423E-04	0.14633E-03	0.18833E-05	0.12527E-04
0.4525E 00	0.62127E-04	0.19488E-03	0.35467E-05	0.17232E-04
0.6400E 00	0.10494E-03	0.25222E-03	0.64941E-05	0.23271E-04
0.9051E 00	0.16934E-03	0.31420E-03	0.11447E-04	0.30569E-04
0.1280E 01	0.25910E-03	0.37276E-03	0.19219E-04	0.38612E-04
0.1810E 01	0.37328E-03	0.41668E-03	0.30409E-04	0.46289E-04
0.2560E 01	0.50397E-03	0.43481E-03	0.44925E-04	0.51978E-04
0.3620E 01	0.63684E-03	0.42106E-03	0.61602E-04	0.54084E-04
0.5120E 01	0.75576E-03	0.37812E-03	0.78339E-04	0.51844E-04
0.7241E 01	0.84926E-03	0.31670E-03	0.92910E-04	0.45848E-04
0.1024E 02	0.91430E-03	0.25026E-03	0.10394E-03	0.37750E-04
0.1448E 02	0.95496E-03	0.18934E-03	0.11131E-03	0.29376E-04
0.2048E 02	0.97836E-03	0.13915E-03	0.11575E-03	0.21970E-04
0.2896E 02	0.99106E-03	0.10047E-03	0.11823E-03	0.16023E-04
0.4096E 02	0.99771E-03	0.71824E-04	0.11955E-03	0.11518E-04
0.5793E 02	0.10011E-02	0.51073E-04	0.12024E-03	0.82133E-05

A= 0.16

ALPHA	H(Z) REAL	H(Z) IMAG	H(RHO) REAL	H(RHO) IMAG
0.5000E-02	0.10C79E-06	0.19716E-04	0.80371E-08	0.31548E-05
0.7071E-02	0.20098E-06	0.27879E-04	0.16072E-07	0.44616E-05
0.1000E-01	0.39990E-06	0.39418E-04	0.32138E-07	0.63094E-05
0.1414E-01	0.79329E-06	0.55724E-04	0.64252E-07	0.89224E-05
0.2000E-01	0.15687E-05	0.78755E-04	0.12841E-06	0.12617E-04
0.2828E-01	0.30936E-05	0.11125E-03	0.25653E-06	0.17840E-04
0.4000E-01	0.60843E-05	0.15704E-03	0.51206E-06	0.25219E-04
0.5657E-01	0.11907E-04	0.22134E-03	0.10208E-05	0.35639E-04
0.8000E-01	0.23101E-04	0.31119E-03	0.20302E-05	0.50329E-04
0.1131E 00	0.44269E-04	0.43577E-03	0.40217E-05	0.70983E-04
0.1600E 00	0.83557E-04	0.60640E-03	0.79161E-05	0.99877E-04
0.2263E 00	0.15473E-03	0.83568E-03	0.15433E-04	0.13995E-03
0.3200E 00	0.27957E-03	0.11350E-02	0.29662E-04	0.19469E-03
0.4525E 00	0.48966E-03	0.15093E-02	0.55840E-04	0.26764E-03
0.6400E 00	0.82541E-03	0.19492E-02	0.10213E-03	0.36108E-03
0.9051E 00	0.13286E-02	0.24208E-02	0.17975E-03	0.47363E-03
0.1280E 01	0.20261E-02	0.28603E-02	0.30118E-03	0.59699E-03
0.1810E 01	0.29073E-02	0.31804E-02	0.47529E-03	0.71355E-03
0.2560E 01	0.39066E-02	0.32971E-02	0.69992E-03	0.79817E-03
0.3620E 01	0.49110E-02	0.31688E-02	0.95619E-03	0.82661E-03
0.5120E 01	0.57977E-02	0.28229E-02	0.12112E-02	0.78823E-03
0.7241E 01	0.64842E-02	0.23462E-02	0.14311E-02	0.69337E-03
0.1024E 02	0.69544E-02	0.18419E-02	0.15959E-02	0.56819E-03
0.1448E 02	0.72443E-02	0.13868E-02	0.17050E-02	0.44050E-03
0.2048E 02	0.74092E-02	0.10159E-02	0.17701E-02	0.32859E-03
0.2896E 02	0.74980E-02	0.73208E-03	0.18064E-02	0.23927E-03
0.4096E 02	0.75443E-02	0.52278E-03	0.18256E-02	0.17183E-03
0.5793E 02	0.75679E-02	0.37153E-03	0.18355E-02	0.12247E-03

A= 0.32

ALPHA	H(Z) REAL	H(Z) IMAG	H(RHO) REAL	H(RHO) IMAG
0.5000E-02	0.77557E-06	0.14153E-03	0.12178E-06	0.45295E-04
0.7071E-02	0.15445E-05	0.20013E-03	0.24353E-06	0.64056E-04
0.1000E-01	0.30705E-05	0.28296E-03	0.48695E-06	0.90587E-04
0.1414E-01	0.60953E-05	0.40001E-03	0.97352E-06	0.12810E-03
0.2000E-01	0.12081E-04	0.56532E-03	0.19458E-05	0.18114E-03
0.2828E-01	0.23877E-04	0.79851E-03	0.38872E-05	0.25612E-03
0.4000E-01	0.46955E-04	0.11268E-02	0.77589E-05	0.36206E-03
0.5657E-01	0.91691E-04	0.15875E-02	0.15463E-04	0.51161E-03
0.8000E-01	0.17745E-03	0.22306E-02	0.30739E-04	0.72240E-03
0.1131E 00	0.33945E-03	0.31206E-02	0.60857E-04	0.10186E-02
0.1600E 00	0.63540E-03	0.43354E-02	0.11970E-03	0.14326E-02
0.2263E 00	0.11804E-02	0.59591E-02	0.23310E-03	0.20057E-02
0.3200E 00	0.21234E-02	0.80609E-02	0.44715E-03	0.27864E-02
0.4525E 00	0.36977E-02	0.10656E-01	0.83935E-03	0.38214E-02
0.6400E 00	0.61849E-02	0.13642E-01	0.15288E-02	0.51361E-02
0.9051E 00	0.98550E-02	0.16736E-01	0.26750E-02	0.66980E-02
0.1280E 01	0.14836E-01	0.19448E-01	0.44468E-02	0.83712E-02
0.1810E 01	0.20950E-01	0.21159E-01	0.69461E-02	0.98888E-02
0.2560E 01	0.27628E-01	0.21353E-01	0.10101E-01	0.10894E-01
0.3620E 01	0.34027E-01	0.19893E-01	0.13603E-01	0.11075E-01
0.5120E 01	0.39357E-01	0.17146E-01	0.16972E-01	0.10346E-01
0.7241E 01	0.43223E-01	0.13810E-01	0.19768E-01	0.89164E-02
0.1024E 02	0.45697E-01	0.10560E-01	0.21784E-01	0.71761E-02
0.1448E 02	0.47132E-01	0.77993E-02	0.23069E-01	0.54866E-02
0.2048E 02	0.47910E-01	0.56427E-02	0.23815E-01	0.40544E-02
0.2896E 02	0.48315E-01	0.40369E-02	0.24221E-01	0.29354E-02
0.4096E 02	0.48522E-01	0.28713E-02	0.24434E-01	0.21013E-02
0.5793E 02	0.48626E-01	0.20363E-02	0.24542E-01	0.14952E-02

A= 0.64

ALPHA	H(Z) REAL	H(Z) IMAG	H(RHO) REAL	H(RHO) IMAG
0.5000E-02	0.54687E-05	0.78303E-03	0.16149E-05	0.50123E-03
0.7071E-02	0.10891E-04	0.11072E-02	0.32293E-05	0.70883E-03
0.1000E-01	0.21667E-04	0.15653E-02	0.64571E-05	0.10024E-02
0.1414E-01	0.43034E-04	0.22125E-02	0.12909E-04	0.14175E-02
0.2000E-01	0.85216E-04	0.31259E-02	0.25798E-04	0.20044E-02
0.2828E-01	0.16802E-03	0.44129E-02	0.51525E-04	0.28338E-02
0.4000E-01	0.32944E-03	0.62216E-02	0.10280E-03	0.40053E-02
0.5657E-01	0.64120E-03	0.87521E-02	0.20473E-03	0.56582E-02
0.8000E-01	0.12355E-02	0.12266E-01	0.40654E-03	0.79851E-02
0.1131E 00	0.23487E-02	0.17087E-01	0.80339E-03	0.11248E-01
0.1600E 00	0.43859E-02	0.23575E-01	0.15755E-02	0.15791E-01
0.2263E 00	0.80011E-02	0.32052E-01	0.30535E-02	0.22036E-01
0.3200E 00	0.14163E-01	0.42632E-01	0.58150E-02	0.30440E-01
0.4525E 00	0.24126E-01	0.54943E-01	0.10798E-01	0.41356E-01
0.6400E 00	0.39183E-01	0.67773E-01	0.19361E-01	0.54756E-01
0.9051E 00	0.60053E-01	0.78848E-01	0.33143E-01	0.69788E-01
0.1280E 01	0.85990E-01	0.85118E-01	0.53495E-01	0.84367E-01
0.1810E 01	0.11412E 00	0.83912E-01	0.80457E-01	0.95212E-01
0.2560E 01	0.13994E 00	0.74643E-01	0.11176E 00	0.98898E-01
0.3620E 01	0.15930E 00	0.59768E-01	0.14296E 00	0.93757E-01
0.5120E 01	0.17070E 00	0.43654E-01	0.16930E 00	0.81237E-01
0.7241E 01	0.17573E 00	0.29985E-01	0.18816E 00	0.65176E-01
0.1024E 02	0.17720E 00	0.20117E-01	0.19987E 00	0.49448E-01
0.1448E 02	0.17732E 00	0.13560E-01	0.20640E 00	0.36250E-01
0.2048E 02	0.17713E 00	0.92782E-02	0.20984E 00	0.26090E-01
0.2896E 02	0.17696E 00	0.64349E-02	0.21159E 00	0.18608E-01
0.4096E 02	0.17685E 00	0.45026E-02	0.21247E 00	0.13213E-01
0.5793E 02	0.17679E 00	0.31664E-02	0.21291E 00	0.93624E-02

A= 1.28

ALPHA	H(Z) REAL	H(Z) IMAG	H(RHO) REAL	H(RHO) IMAG
0.5000E-02	0.31860E-04	0.24456E-02	0.15739E-04	0.31317E-02
0.7071E-02	0.63410E-04	0.34572E-02	0.31472E-04	0.44287E-02
0.1000E-01	0.12593E-03	0.48856E-02	0.62921E-04	0.62627E-02
0.1414E-01	0.24934E-03	0.69001E-02	0.12576E-03	0.88553E-02
0.2000E-01	0.49166E-03	C.97350E-02	0.25120E-03	0.12519E-01
0.2828E-01	0.96416E-03	0.13710E-01	0.50131E-03	0.17694E-01
0.4000E-01	0.18764E-02	0.19248E-01	0.99880E-03	0.24994E-01
0.5657E-01	0.36137E-02	0.26881E-01	0.19845E-02	0.35266E-01
0.8000E-01	0.68612E-02	C.37219E-01	0.39251E-02	0.49658E-01
0.1131E 00	0.12779E-01	0.50818E-01	0.77062E-02	0.69658E-01
0.1600E 00	0.23191E-01	C.67873E-01	0.14955E-01	0.97057E-01
0.2263E 00	0.40662E-01	C.87603E-01	0.28515E-01	0.13366E 00
0.3200E 00	0.68121E-01	0.10731E 00	0.52970E-01	0.18051E 00
0.4525E 00	0.10754E 00	0.12142E 00	0.94813E-01	0.23635E 00
0.6400E 00	0.15726E 00	0.12144E 00	0.16131E 00	0.29526E 00
0.9051E 00	0.20884E 00	0.98809E-01	0.25680E 00	0.34481E 00
0.1280E 01	0.24656E 00	0.51268E-01	0.37662E 00	0.36776E 00
0.1810E 01	0.25411E 00	-0.10389E-01	0.50264E 00	0.35028E 00
0.2560E 01	0.22720E 00	-0.64183E-01	0.60850E 00	0.29398E 00
0.3620E 01	0.18003E 00	-0.91471E-01	0.67570E 00	0.21894E 00
0.5120E 01	0.13445E 00	-0.90995E-01	0.70587E 00	0.14998E 00
0.7241E 01	0.10292E 00	-0.75396E-01	0.71436E 00	0.99659E-01
0.1024E 02	0.85147E-01	-0.57043E-01	0.71497E 00	0.66823E-01
0.1448E 02	0.76056E-01	-C.41487E-01	0.71403E 00	0.45700E-01
0.2048E 02	0.71536E-01	-0.29696E-01	0.71323E 00	0.31730E-01
0.2896E 02	0.69293E-01	-C.21116E-01	0.71274E 00	0.22225E-01
0.4096E 02	0.68178E-01	-0.14971E-01	0.71248E 00	0.15640E-01
0.5793E 02	0.67622E-01	-0.10600E-01	0.71235E 00	0.11032E-01

A= 2.56

ALPHA	H(Z) REAL	H(Z) IMAG	H(RHO) REAL	H(RHO) IMAG
0.5000E-02	0.14939E-03	0.40321E-02	0.10417E-03	0.10343E-01
0.7071E-02	0.29619E-03	0.56921E-02	0.20824E-03	0.14625E-01
0.1000E-01	0.58511E-03	0.80241E-02	0.41612E-03	0.20677E-01
0.1414E-01	0.11502E-02	0.11283E-01	0.83097E-03	0.29227E-01
0.2000E-01	0.22455E-02	0.15795E-01	0.16574E-02	0.41290E-01
0.2828E-01	0.43415E-02	0.21944E-01	0.32990E-02	0.58276E-01
0.4000E-01	0.82822E-02	0.30093E-01	0.65435E-02	0.82097E-01
0.5657E-01	0.15508E-01	0.40368E-01	0.12904E-01	0.11525E 00
0.8000E-01	0.28294E-01	0.52161E-01	0.25206E-01	0.16077E 00
0.1131E 00	0.49797E-01	0.63165E-01	0.48504E-01	0.22173E 00
0.1600E 00	0.83358E-01	0.67826E-01	0.91206E-01	0.29982E 00
0.2263E 00	0.13006E 00	0.55673E-01	0.16569E 00	0.39222E 00
0.3200E 00	0.18352E 00	0.11425E-01	0.28636E 00	0.48645E 00
0.4525E 00	0.22311E 00	-0.79097E-01	0.46178E 00	0.55523E 00
0.6400E 00	0.21261E 00	-0.21375E 00	0.67919E 00	0.55900E 00
0.9051E 00	0.11739E 00	-0.35631E 00	0.89057E 00	0.46715E 00
0.1280E 01	-0.58424E-01	-0.44209E 00	0.10258E 01	0.29453E 00
0.1810E 01	-0.25278E 00	-0.42708E 00	0.10458E 01	0.11264E 00
0.2560E 01	-0.39169E 00	-0.33599E 00	0.98524E 00	-0.43902E-02
0.3620E 01	-0.45661E 00	-0.23366E 00	0.91385E 00	-0.45060E-01
0.5120E 01	-0.47788E 00	-0.15745E 00	0.86761E 00	-0.45547E-01
0.7241E 01	-0.48391E 00	-0.10756E 00	0.84403E 00	-0.35818E-01
0.1024E 02	-0.48584E 00	-0.74659E-01	0.83264E 00	-0.26314E-01
0.1448E 02	-0.48657E 00	-0.52303E-01	0.82710E 00	-0.18908E-01
0.2048E 02	-0.48689E 00	-0.36812E-01	0.82437E 00	-0.13469E-01
0.2896E 02	-0.48704E 00	-0.25970E-01	0.82301E 00	-0.95578E-02
0.4096E 02	-0.48711E 00	-0.18343E-01	0.82234E 00	-0.67701E-02
0.5793E 02	-0.48715E 00	-0.12963E-01	0.82200E 00	-0.47913E-02

A= 5.12

ALPHA	H(Z) REAL	H(Z) IMAG	H(RHO) REAL	H(RHO) IMAG
0.5000E-02	0.61759E-03	0.46666E-02	0.52889E-03	0.24189E-01
0.7071E-02	0.12147E-02	0.65306E-02	0.10564E-02	0.34189E-01
0.1000E-01	0.23728E-02	0.90631E-02	0.21078E-02	0.48299E-01
0.1414E-01	0.45903E-02	0.12393E-01	0.41978E-02	0.68161E-01
0.2000E-01	0.87601E-02	0.16504E-01	0.83342E-02	0.96003E-01
0.2828E-01	0.16398E-01	0.20939E-01	0.16458E-01	0.13472E 00
0.4000E-01	0.29868E-01	0.24159E-01	0.32215E-01	0.18774E 00
0.5657E-01	0.52311E-01	0.22315E-01	0.62164E-01	0.25836E 00
0.8000E-01	0.86557E-01	0.73260E-02	0.11727E 00	0.34772E 00
0.1131E 00	0.13160E 00	-0.35128E-01	0.21371E 00	0.45032E 00
0.1600E 00	0.17519E 00	-0.12491E 00	0.36979E 00	0.54652E 00
0.2263E 00	0.18410E 00	-0.27782E 00	0.59371E 00	0.59499E 00
0.3200E 00	0.10353E 00	-0.48131E 00	0.85865E 00	0.53764E 00
0.4525E 00	-0.11184E 00	-0.66650E 00	0.10807E 01	0.33692E 00
0.6400E 00	-0.43218E 00	-0.72420E 00	0.11470E 01	0.40348E-01
0.9051E 00	-0.72705E 00	-0.60315E 00	0.10207E 01	-0.20842E 00
0.1280E 01	-0.87524E 00	-0.39201E 00	0.81031E 00	-0.29379E 00
0.1810E 01	-0.89361E 00	-0.22393E 00	0.65546E 00	-0.24996E 00
0.2560E 01	-0.87285E 00	-0.13338E 00	0.58406E 00	-0.17824E 00
0.3620E 01	-0.85709E 00	-0.86821E-01	0.55614E 00	-0.12351E 00
0.5120E 01	-0.84903E 00	-0.59222E-01	0.54431E 00	-0.86207E-01
0.7241E 01	-0.84507E 00	-0.41185E-01	0.53883E 00	-0.60554E-01
0.1024E 02	-0.84312E 00	-0.28889E-01	0.53618E 00	-0.42676E-01
0.1448E 02	-0.84214E 00	-0.20347E-01	0.53487E 00	-0.30127E-01
0.2048E 02	-0.84166E 00	-0.14359E-01	0.53423E 00	-0.21285E-01
0.2896E 02	-0.84142E 00	-0.10144E-01	0.53391E 00	-0.15045E-01
0.4096E 02	-0.84130E 00	-0.71691E-02	0.53375E 00	-0.10636E-01
0.5793E 02	-0.84124E 00	-0.50681E-02	0.53367E 00	-0.75200E-02

A=10.24

ALPHA	H(Z) REAL	H(Z) IMAG	H(RHO) REAL	H(RHO) IMAG
0.5000E-02	0.24070E-02	0.45266E-02	0.23549E-02	0.50360E-01
0.7071E-02	0.46557E-02	0.59616E-02	0.46911E-02	0.71060E-01
0.1000E-01	0.88805E-02	0.73667E-02	0.93166E-02	0.10006E 00
0.1414E-01	0.16604E-01	0.79083E-02	0.18407E-01	0.14033E 00
0.2000E-01	0.30168E-01	0.54592E-02	0.36055E-01	0.19534E 00
0.2828E-01	0.52567E-01	-0.47650E-02	0.69628E-01	0.26822E 00
0.4000E-01	0.86078E-01	-0.32329E-01	0.13145E 00	0.35932E 00
0.5657E-01	0.12799E 00	-0.93676E-01	0.23955E 00	0.46095E 00
0.8000E-01	0.16181E 00	-0.21083E 00	0.41374E 00	0.54834E 00
0.1131E 00	0.14589E 00	-0.39900E 00	0.66000E 00	0.57093E 00
0.1600E 00	0.14219E-01	-0.63585E 00	0.93916E 00	0.45996E 00
0.2263E 00	-0.28109E 00	-0.82749E 00	0.11404E 01	0.17874E 00
0.3200E 00	-0.68300E 00	-0.83630E 00	0.11246E 01	-0.19248E 00
0.4525E 00	-0.10068E 01	-0.62066E 00	0.87261E 00	-0.45346E 00
0.6400E 00	-0.11115E 01	-0.33342E 00	0.56447E 00	-0.47468E 00
0.9051E 00	-0.10670E 01	-0.15069E 00	0.38164E 00	-0.35115E 00
0.1280E 01	-0.10113E 01	-0.78280E-01	0.31847E 00	-0.23289E 00
0.1810E 01	-0.98281E 00	-0.49350E-01	0.29967E 00	-0.15713E 00
0.2560E 01	-0.96991E 00	-0.33441E-01	0.29247E 00	-0.10868E 00
0.3620E 01	-0.96382E 00	-0.23201E-01	0.28920E 00	-0.76052E-01
0.5120E 01	-0.96085E 00	-0.16257E-01	0.28763E 00	-0.53505E-01
0.7241E 01	-0.95938E 00	-0.11444E-01	0.28686E 00	-0.37740E-01
0.1024E 02	-0.95865E 00	-0.80743E-02	0.28648E 00	-0.26653E-01
0.1448E 02	-0.95829E 00	-0.57031E-02	0.28629E 00	-0.18835E-01
0.2048E 02	-0.95811E 00	-0.40305E-02	0.28619E 00	-0.13314E-01
0.2896E 02	-0.95801E 00	-0.28492E-02	0.28615E 00	-0.94130E-02
0.4096E 02	-0.95797E 00	-0.20144E-02	0.28612E 00	-0.66555E-02
0.5793E 02	-0.95795E 00	-0.14243E-02	0.28611E 00	-0.47060E-02

A=20.48

ALPHA	H(Z) REAL	H(Z) IMAG	H(RHO) REAL	H(RHO) IMAG
0.5000E-02	0.89C51E-02	0.24457E-02	0.98198E-02	0.10109E 00
0.7071F-02	0.16636E-01	0.89438E-03	0.19405E-01	0.14173E 00
0.1000E-01	0.3C173E-01	-0.45955E-02	0.38018E-01	0.19714E 00
0.1414E-01	0.52398E-01	-C.19300E-01	0.73438E-01	0.27027E 00
0.2000E-01	0.85215E-01	-C.53548E-01	0.13866E 00	0.36095E 00
0.2828E-01	0.12490E 00	-C.12484E 0C	0.25259E 00	0.46011E 00
0.4000E-01	0.15248E 00	-0.25613E 00	0.43553E 00	0.54001E 00
0.5657E-01	0.12155E 00	-0.46175E 0C	0.69161E 00	0.54494E 00
0.8000E-01	-0.39743E-01	-0.71289E 00	0.97368E 00	0.40073E 00
0.1131E 00	-0.37891E 00	-0.90C58E 00	0.11548E 01	0.73283E-01
0.1600E 00	-0.81991E 00	-C.87219E 00	0.10826E 01	-0.33472E 00
0.2263E 00	-0.11451E 01	-C.59780E 00	0.75475E 00	-0.58917E 00
0.3200E 00	-0.12092F 01	-C.27370E 0C	0.39867E 00	-0.56024E 00
0.4525E 00	-0.11232E 01	-C.95527E-01	0.21380E 00	-0.38855E 00
0.6400E 00	-0.10499E 01	-0.41625E-01	0.16372E 00	-0.24919E 00
0.9051E 00	-0.10169E 01	-C.25507E-01	0.15274E 00	-0.16657E 00
0.1280E 01	-0.1CC25E 01	-C.17245F-01	0.14894E 00	-0.11493E 00
0.1810E 01	-0.99580E 00	-0.11956E-01	0.14723E 00	-0.80354E-01
0.2560E 01	-0.99253E 0C	-0.83753F-02	0.14641E 00	-0.565C8E-01
0.3620E 01	-0.990S2E 00	-0.58951E-02	0.14601E 00	-0.39849E-01
0.5120E 01	-0.99012E 00	-0.41590E-02	0.14581F 00	-0.28140E-01
0.7241E 01	-0.98972E 0C	-C.29375E-02	0.14571E 00	-0.19885E-01
0.1024E 02	-0.98952E 00	-0.2C760E-02	0.14566E 00	-0.14056E-01
0.1448E 02	-0.98942E 0C	-0.14675F-02	0.14564E 00	-0.99374E-02
0.2048E 02	-0.98937E 0C	-C.1C375E-02	0.14563E 00	-0.70262E-02
0.2896E 02	-0.98935E 0C	-0.73361E-03	0.14562E 00	-0.49681E-02
0.4C96E 02	-0.98934E 0C	-0.51872E-03	0.14562E 00	-0.35129E-02
0.5793E 02	-0.98933E 00	-C.36678E-03	0.14562E 00	-0.24840F-02